The [$^2H_8$]THF Radical Cation in CF_3CCl_3 and $CFCl_3$. An EPR and ENDOR Study

Mikael Lindgren,* Roland Erickson, Nikolas P. Benetis and Oleg N. Antzutkin
Chemical Physics, Department of Physics and Measurement Technology, Linköping University of Technology, S-581 83 Linköping, Sweden

The structure and dynamics of the radical cation of deuteriated tetrahydrofuran ([$^2H_8$]THF) stabilized in the freon matrices $CFCl_3$ and CF_3CCl_3 have been investigated by means of EPR and ENDOR spectroscopy. The EPR and ENDOR results of the rigid structure give two pairs of strongly interacting β-deuterium hf splittings [a_D = 1.36 (2 D) and a_D = 0.60 mT (2 D)] consistent with the protonated analogue [Kubodera *et al.*, *J. Phys. Chem.*, 1981, **85**, 2583 (ref. 1)]. An additional hf splitting (0.9–1.1 mT) assigned to the matrix fluorine was resolved above *ca.* 110 K in $CFCl_3$. The temperature dependent EPR lineshapes (77–145 K) involving the exchange between four coupled (I = 1) nuclei have been analysed. A two-site model explained qualitatively the alterating line-widths at intermediate temperatures and resulted in an activation energy of *ca.* 1.7 kcal mol^{-1} A non-perturbative approach adopting a four-site model to account for puckering motion was tested. The dynamics were also manifested as a reversible temperature effect for the ENDOR. The relative abundance of resonances due to an averaged (hf) structure become predominant as the temperature is increased.

A method of studying radical cations of saturated hydrocarbons for the purpose of EPR spectroscopy was introduced together with the halocarbon matrix isolation technique at the end of the seventies.[2–6] Usually only EPR or FDMR are used to characterise the electronic structure of saturated radical cations although methods of higher resolution, such as ENDOR and ESE, are used in many laboratories. Indeed, such ENDOR and ESE studies have only been reported in rare cases[7] and the short-coming of these methods might be attributable to unfavourable relaxation phenomena in combination with inhomogeneous line-broadening.

Cations of saturated five-membered ring structures have attracted attention because of the possibility of ring-inversions and puckering motions having relatively small activation energies, say, 1–2 kcal mol^{-1}.[8] Thus, the low activation barrier would increase the possibility of reaching a 'liquid solution' situation with unresolved anisotropy averaged out, resulting in narrower lines in the EPR and associated ENDOR spectra. In this study line-width discrimination is further enhanced by the use of deuteriated solute molecules. As will be shown, ENDOR lines of the perdeuteriated tetrahydrofuran cation radical can thus be detected at the rigid limit and during rapid exchange. The ENDOR parameters obtained at the rigid limit are consistent with those obtained from EPR line-shape simulations of rigid structures and in dynamic modelling.

From the bulk of experimental data (dynamic EPR, ENDOR) it is also possible to simulate the rigid-limit EPR spectrum of the protonated analogue with high accuracy treating only the anisotropy of the g-factor and dipolar hyperfine tensors as parameters.

The THF radical cation discussed in this paper was first studied by Shida and co-workers,[1] using the $CFCl_3$ matrix, who adopted a two-site exchange model to account for the line-width alterations observed on varying the sample temperature between 77 and 150 K. A four-site model which can account for exchange between C_s and C_2 structures has been tested in this study and is discussed. With this model it is possible to examine specific paths within the pseudorotational potential. The two-site model was found to be adequate for the deuteriated cation radical and we conclude that the cation radical prefers two-site jumping between two identical C_2 (or C_s) structures at low temperature and that populations of other configurations are not prominent in the temperature region examined (77–150 K). This supports earlier assumptions in studies of cations of saturated five-membered rings.

Experimental

The solutes and matrices were commercially available (Aldrich) and used without further purification. The solutes were mixed with the matrix (< 1 mol%) on a vacuum line using standard techniques. The radical cations were generated at 77 K by X-ray irradiation. This is a well established method of generating and stabilizing the solute radical cation. The EPR spectra were recorded using a Bruker ER200/ESP300 spectrometer.

The simulation of the two-site model was accomplished using a program originally developed by Heinzer[9] for chemical exchange of isotropic systems, but modified by Sjöqvist *et al.*[8] to account for anisotropic hf interactions and g-values.

The spectral simulations of the 4-site models based on conventional theory of chemical exchange in the Kaplan–Alexander regime has been developed by Benetis *et al.*[10] The current version of the program handles a maximum of six coupled nuclei in six sites of arbitrary anisotropy (Zeeman, hyperfine, quadrupolar) in the spin Hamiltonian. A typical spectrum of the radicals discussed in this report, *i.e.*, four sites and four coupled isotropic nuclei (I = 1), takes about 15 min to calculate using a VAX mini-computer. The introduction of g-anisotropy requires an integration routine (summation) of spectra at different orientations which makes the calculation times substantially longer. Twenty-five spectra, each being a superposition of four sites *via* the exchange process, were enough to produce a random 'powder' pattern. A short review of the methodology of simulating exchange-broadened spectra are given below; for further details see ref. 10.

Lineshape theory.—In the non-perturbative approach, the theoretical absorption signal is defined as the real part of

$$\langle S_+(\Omega,\omega)\rangle = S'_+[\boldsymbol{R} + i\cdot(L^d(\Omega) - l\omega)]^{-1}\rho'_0$$

with

$$\boldsymbol{L}^{d} = \boldsymbol{Z}^{-1}\boldsymbol{L}\boldsymbol{Z}$$

$$\boldsymbol{S}'_{+} = \boldsymbol{S}_{+}\boldsymbol{Z}$$

$$\rho' = \boldsymbol{Z}^{-1}\rho_0$$

for some orientation Ω

$\boldsymbol{R}$ is the relaxation matrix

$\boldsymbol{L}^{d}$ is obtained by diagonalizing the Liouville superoperator $\boldsymbol{L}$

$\boldsymbol{Z}$ is the transformation matrix diagonalizing $\boldsymbol{L}$

The density operator is given by the direct product

$$\rho_o = \rho_o \cdot \boldsymbol{P}_{ss}$$

where $\boldsymbol{P}_{ss}$ is a vector containing the steady-state population of each site and ρ_0 is the density operator of the total spin after a 90° pulse.

The Liouville operator $\boldsymbol{L}$ contains the spin Hamiltonian $\boldsymbol{H}^{x}$ and the exchange part Γ which is obtained by considering a reorganisation of the system

$$\boldsymbol{L} = \begin{pmatrix} \boldsymbol{H}^{x[1]} & 0 & 0 & 0 \\ 0 & \boldsymbol{H}^{x[2]} & 0 & 0 \\ 0 & 0 & \boldsymbol{H}^{x[3]} & 0 \\ 0 & 0 & 0 & \boldsymbol{H}^{x[4]} \end{pmatrix} + \mathrm{i}\cdot \begin{pmatrix} \Gamma_{11}\mathrm{I} & \Gamma_{12}\mathrm{I} & \Gamma_{13}\mathrm{I} & \Gamma_{14}\mathrm{I} \\ \Gamma_{21}\mathrm{I} & \Gamma_{22}\mathrm{I} & \Gamma_{23}\mathrm{I} & \Gamma_{24}\mathrm{I} \\ \Gamma_{31}\mathrm{I} & \Gamma_{32}\mathrm{I} & \Gamma_{33}\mathrm{I} & \Gamma_{34}\mathrm{I} \\ \Gamma_{41}\mathrm{I} & \Gamma_{42}\mathrm{I} & \Gamma_{43}\mathrm{I} & \Gamma_{44}\mathrm{I} \end{pmatrix}$$

The Dynamical Model.—All configurations with interchanged scalar constants and/or tensor orientations (isotropic and anisotropic interactions) are considered as different sites. The population of each site varies according to

$$\frac{d\boldsymbol{P}}{dt} = \Gamma \cdot \boldsymbol{P} \text{ where } \Gamma \cdot \boldsymbol{P} = \begin{pmatrix} \Gamma_{11} & \Gamma_{12} & \Gamma_{13} & \Gamma_{14} \\ \Gamma_{21} & \Gamma_{22} & \Gamma_{23} & \Gamma_{24} \\ \Gamma_{31} & \Gamma_{32} & \Gamma_{33} & \Gamma_{34} \\ \Gamma_{41} & \Gamma_{42} & \Gamma_{43} & \Gamma_{44} \end{pmatrix} \begin{pmatrix} P_1 \\ P_2 \\ P_3 \\ P_4 \end{pmatrix}$$

The exchange operator Γ is a Markov operator obtained phenomenologically from the rate constants. For the pair of sites $[i][j]$, the rate constants of the two opposite transitions k_{ji} and k_{ij} are introduced in Γ as the non-diagonal matrix elements Γ_{ij} and Γ_{ji}, respectively. Conservation of the populations for a closed system implies

$$\frac{d\,\Sigma_j P_j}{dt} = 0$$

for all values of the populations P_j which gives the following relation for the diagonal matrix elements of Γ

$$\Gamma_{ii} = -\sum_{j \neq i} \Gamma_{ji}$$

The steady-state populations ($d\boldsymbol{P}/dt = 0$) are input parameters for calculating the EPR spectrum. They can be obtained as

$$\boldsymbol{P}_{ss} = \frac{1}{|Y_{1i}| + |Y_{2i}| + |Y_{3i}| + |Y_{4i}|} \begin{pmatrix} Y_{1i} \\ Y_{2i} \\ Y_{3i} \\ Y_{4i} \end{pmatrix}$$

where Y is the transformation diagonalizing Γ and index i is that corresponding to the zero eigenvalue.

Results and Discussions

Experimental EPR Spectra and Electronic Ground State of the $[^2H_8]$*THF Cation.*—The experimental EPR spectra of the $[^2H_8]$ THF cation radical formed by irradiation at 77 K in a CF_3CCl_3 matrix and measured in the temperature range 77–142 K are shown in Fig. 1(*a*). In the rigid limit, the spectrum is a quintet of quintets with hyperfine interaction to two sets of pairwise equivalent deuterium splittings ($I = 1$) of *ca.* 1.36 and 0.6 mT. Keeping the sample temperature *ca.* 100–120 K one observes the characteristic line-width alteration in the spectra implying dynamical exchange between the two sets of nuclei having different hyperfine couplings. Similar spectra are obtained using the $CFCl_3$ matrix, however, with the addition of a doublet as the temperature becomes higher, Fig. 1(*b*). The origin of this doublet we assign to hyperfine interaction with matrix fluorine (apparent hf coupling constant in the range 0.9–1.2 mT depending on the temperature) and this will be discussed later.

The spectra obtained at the rigid limit is consistent with earlier results of Shida *et al.*,[1] who studied the protonated analogue, if we rescale the hyperfine splittings with the appropriate gyromagnetic ratio nuclear spin quantum number ($I = 1$) for deuterium.

Deuterium HF Splittings Detected by ENDOR Spectroscopy.—ENDOR spectra of the perdeuteriated THF cation in $CFCl_3$ recorded at two different temperatures are shown in Fig. 2, and correspond to the rigid limit and fast exchange limits, respectively. The spectra are obtained by pumping the centre line of the EPR spectrum. The same (but weaker) ENDOR spectra are obtained by pumping lines associated with other (total) spin quantum numbers.

Frequencies of apparent ENDOR lines are given in the spectra. At low temperature, 105 K, four lines are detected associated with the smaller β-splitting due to the equatorial position[1] (6.27–11.41 MHz). This corresponds to an EPR hf splitting of 17.08 MHz (0.61 mT) and 18.38 MHz (0.65 mT). A strong response is obtained from distant matrix fluorine (13.72 MHz), and a very weak feature can be discerned at 16.59 MHz. The latter is the low-frequency line due to the hf splitting of the axially positioned deuterium in the β-position (37.65 MHz or 1.34 mT). No high-frequency line associated to this hf splitting could be observed.

At the higher temperature (128 K) the ENDOR spectrum has changed. Small shifts of the frequencies associated with the smaller deuterium splittings (5.98—*ca.* 11.51 MHz) are observed. This is probably due to the motions of the cation; the associated EPR spectrum [Fig. 1(*b*)] corresponds to a cation nearly in the fast exchange limit (in the deuterium hf splitting timescale). There are two new deuterium lines, at 11.51 and 16.12 MHz, which is the effective hyperfine splitting one obtains by averaging the β-splittings of the axial and equatorial deuteriums at the rigid limit (27.63 MHz or 0.98 mT).

The hyperfine couplings obtained from ENDOR were consistent with the EPR hyperfine patterns which were investigated in detail from dynamical line-shape simulations to be described in following sections. The hf splitting and *g*-value parameters of the rigid cation deduced from ENDOR and EPR are all collected in Table 1.

Matrix HF Interactions.—The EPR spectrum obtained for the protonated THF cation radical at 127 K in two different matrices, CF_3CCl_3 and $CFCl_3$, are shown in Fig. 3. Here one can clearly see an additional splitting of the outermost lines using the $CFCl_3$ matrix. Both protonated and deuteriated THF cation radicals give this additional splitting using the $CFCl_3$ matrix (*ca.* 1.0 mT at 130 K), and thus, it seems reasonable to assign this doublet to hf interaction with a fluorine atom of the matrix. Attempts to obtain conclusive evidence for this assignment by ENDOR spectroscopy failed. However, several lines in the (temperature-dependent) ENDOR spectra could not

Table 1 The g-tensor and hf parameters obtained for $[^2H_8]THF^+$ and THF^+ in $CFCl_3$

Isotope in radical	T/K	g-tensor and Euler angles	Hyperfine couplings /mT[a]	Type of investigation
D	77		$a_1^D = a_2^D = 1.36$ $a_3^D = a_4^D = 0.60$	EPR
D	105		$a_1^D = 0.61$ $a_2^D = 0.65$ $a_3^D = 1.34 = a_4^D$? $a_m^F = 0.0$ = distant matrix fluorine	ENDOR
D	128		$a_1^D = 0.6$ $a_{av}^D = 0.98$	ENDOR
D and H	>110		$a^F = 0.9$–1.1	EPR
H	77	$g_x = 2.0023$ $\alpha = 0.0$ $g_y = 2.0037$ $\beta = 175.4$ $g_z = 2.0062$ $\gamma = -90.0$	$A_x = 4.29\ h_1 = (6.2, 104.4, 27.1)$ $A_y = 3.82\ h_2 = (6.2, 75.6, -27.1)$ $A_z = 3.78$ $A_x = 9.15\ h_3 = (-39.3, 100.9, 49.8)$ $A_y = 8.68\ h_4 = (-39.3, 79.1, -49.8)$ $A_z = 8.67$ $a(2\ H) = 0.39$ = γ-hydrogen hfc	EPR

[a] a denotes isotropic hf couplings. A denotes principal values of an anisotropic proton hf tensor. Numbers in parentheses, $h_i = (\alpha, \beta, \gamma)$, denotes corresponding Euler angles of proton i.

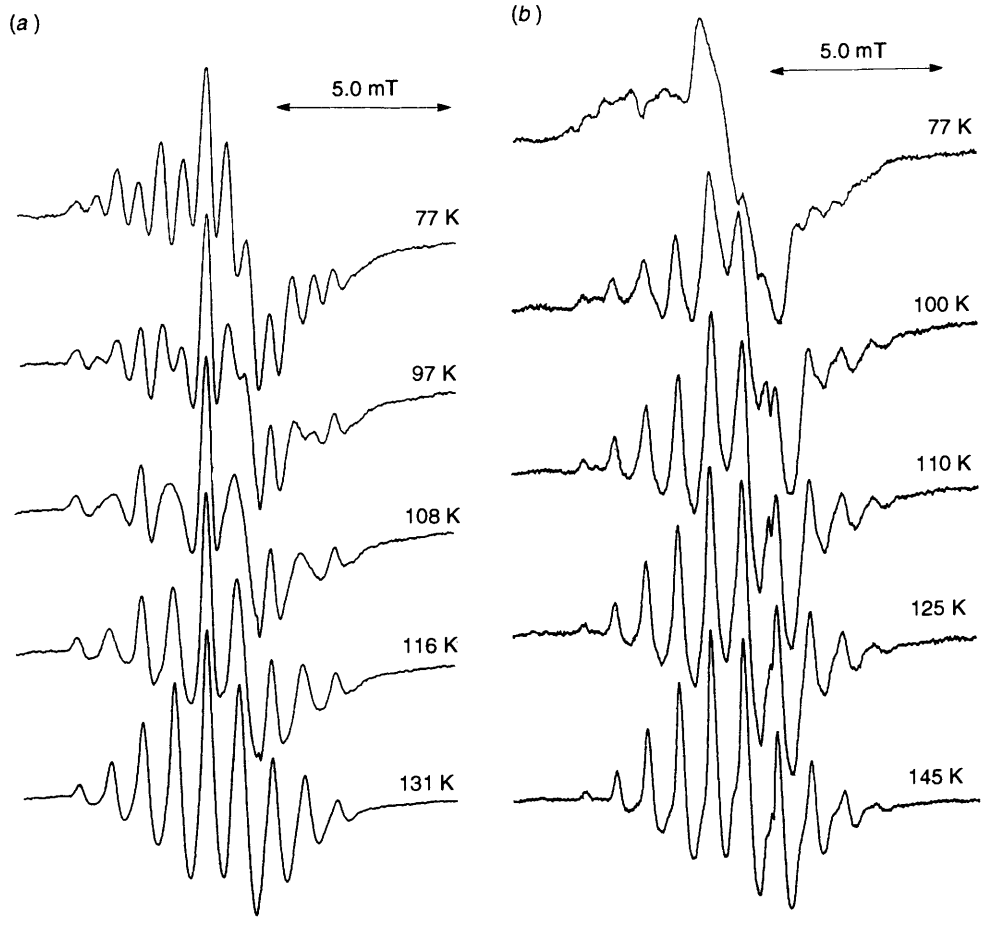

Fig. 1 X-Band EPR spectra of the perdeuteriated THF radical cation in (*a*) CF_3CCl_3 and (*b*) $CFCl_3$, at different temperatures. An irreversible temperature effect was initially observed for the spectra obtained in $CFCl_3$ on going from 77 to *ca.* 150 K (first warming). Subsequent freeze–warm–freeze cycles (4 K–140 K) showed a spectrum identical with that obtained in CF_3CCl_3 at 77 K as the rigid limit.

be explained by deuterium hf couplings. Two such lines are indicated in Fig. 2(*b*). Conclusively, the THF radical cation gives an additional splitting due to matrix fluorine which becomes apparent at higher temperature. This splitting was not

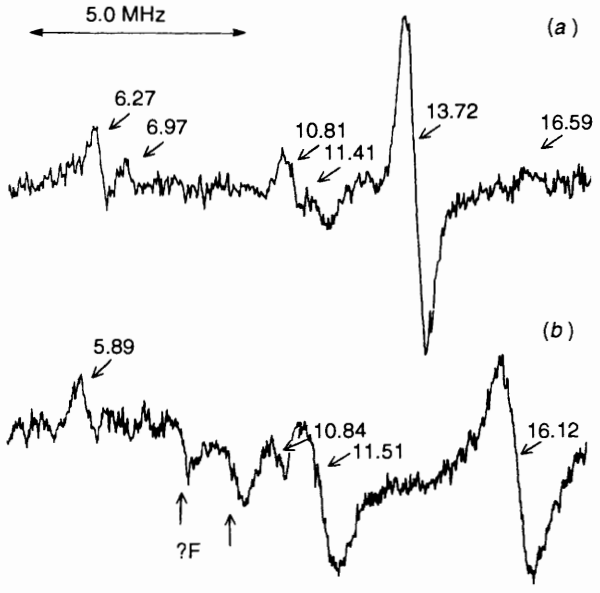

Fig. 2 ENDOR spectra of the perdeuteriated THF radical cation in $CFCl_3$ at two different temperatures, 105 K (*a*) and 128 K (*b*). The spectrum recorded at the lower temperature shows the deuterium ENDOR frequencies associated wih the smaller pair of β splittings (*ca.* 0.6 mT) of the rigid conformation. One frequency of the larger splitting could be detected. The largest peak is the unresolved signal due to matrix fluorine. At the higher temperature the lines associated with an averaged structure (on the hyperfine timescale) predominates. The frequencies are indicated in MHz; further details of assignments are discussed in the text.

observed using CF_3CCl_3 as the matrix. It appears to be a unique property of the $CFCl_3$ matrix.*

Modelling of the Cation Dynamics.—As indicated in the introduction, the saturated five-membered ring molecules have a very shallow potential with respect to puckering of the ring. A rigid structure could in principle be either a C_2 (twisted) or C_s (envelope) or structure of lower symmetry, controlled by the intermolecular forces to the surrounding frozen matrix. Previous studies of the THF cation radical[1] as well as our results on the perdeuteriated analogue shows definitely that the hyperfine splittings to β-hydrogens (deuterium atoms) appears pairwise. Thus, structures of symmetry lower than C_s or C_2 must be ruled out in the rigid limit.

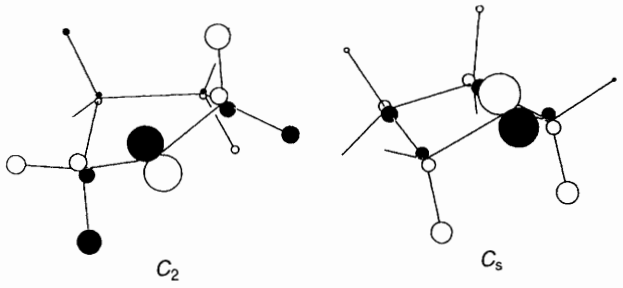

Scheme 1 The SOMO of the C_2 and C_s structures of the tetrahydrofuran (THF) cation radical

The two-site model adopted by Shida *et al.*[1] to account for the dynamics of THF^+ explains the line-width alteration effect. In Fig. 4 simulated spectra at selected rates are shown for the perdeuteriated THF cation in the CF_3CCl_3 matrix (for details of parameters, see Table 2). The associated Arrhenius plot gives the activation energy (Fig. 6). The plot has a tendency to be non-linear and one can extract two activation energies, 1.45 and 2.0 kcal mol^{-1}, if the data are separated in high and low temperature regions, respectively. One cannot discriminate whether the dynamics are caused by exchange between structures having C_2 or C_s symmetry from simulations using isotropic hyperfine splittings and *g*-factors.

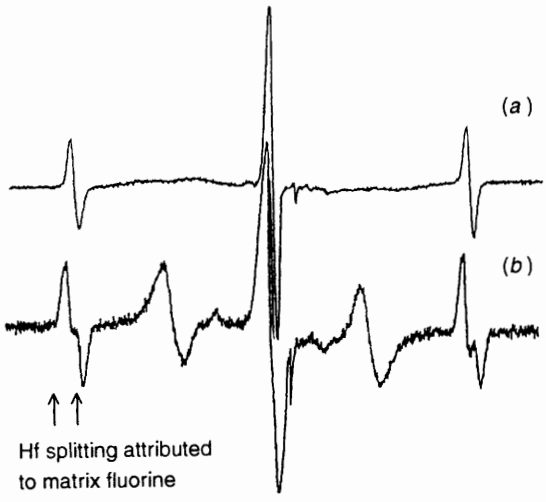

Fig. 3 EPR spectra of the protonated THF cation radical (*a*) at 127 K in CF_3CCl_3; (*b*) at 128 K in $CFCl_3$ (lower). The $CFCl_3$ case shows the appearance of a doublet attributed to matrix fluorine. (Note that the spectra are recorded at a temperature at which the hyperfine interaction of the protons are exchanging causing severe broadening of certain lines. See ref. 1 for a full discussion of related spectra in the temperature range 77 K–155 K).

The reversible EPR line-shape of the cation in two matrices can also be simulated adopting a four-site model as shown below:

Schematic describing the four-site process near the radical centre

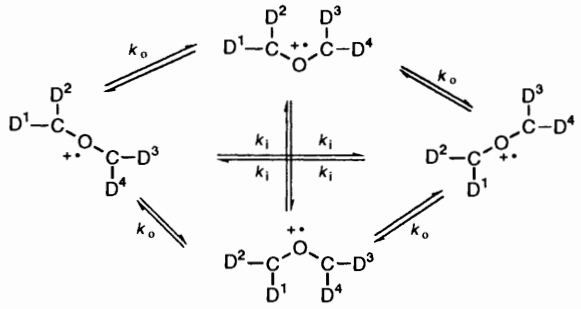

Exchange matrix Γ =

x	k_o	k_i	k_o
k_o	x	k_o	k_i
k_i	k_o	x	k_o
k_o	k_i	k_o	x

In the four-site model we distinguish between two extreme cases: (*i*) exchange taking place between mirror-image C_2 and C_s structures (only), that is, along with the rates labelled k_i above and (*ii*) exchange from C_2 (C_s) to C_2' (C_s') taking place *via* either the C_s (C_2) or C_s' (C_2'), rates labelled k_o above. Although it is possible to have different rates along any of the paths in the scheme above we compare only these two cases. This means that the energies and barriers between all sites for the two models are treated equally (apart from the path which

* It should be noted in this context that we are presently investigating this matrix effect in a series of deuteriated aromatic radical cations using combined ENDOR and ESE methods. The fluorine splitting varies (say 0–0.5 mT), which we believe depends on delocalization of the SOMO of the cation as well as the ionization potential of the solute molecule. Furthermore, Gerson and Qin have observed ^{19}F ENDOR lines in studies of naphthalene in $CFCl_3$.[7a]

Table 2 The g- and hf tensor parameters employed in the simulation of $[^2H_8]THF^+$ dynamics in CF_3CCl_3

Model	Molecular structure (site No.)	g-tensor principal values	hfc/mT[a]	Angle between sites/Euler angles (α, β, γ)/(deg)[b]
Two-site		$g_\perp = 2.006$ $g_\parallel = 2.002$	$A_{1\perp}(2\,D) = 1.33$ $A_{1\parallel}(2\,D) = 1.37$ $A_{2\perp}(2\,D) = 0.61$ $A_{2\parallel}(2\,D) = 0.58$	60
Four-site	C_2(I)	$g_x = 2.0023$ $g_y = 2.0037$ $g_z = 2.0062$	$a_1 = 0.573$ $a_2 = 1.375$ $a_3 = 0.573$ $a_4 = 1.375$	(0.0, 165.4, −90.0)
	C_2(III)	$g_x = 2.0023$ $g_y = 2.0037$ $g_z = 2.0062$	$a_1 = 1.375$ $a_2 = 0.573$ $a_3 = 1.375$ $a_4 = 0.573$	(0.0, 4.6, −90.0)
	C_s(II)	$g_x = 2.0023$ $g_y = 2.0037$ $g_z = 2.0062$	$a_1 = 0.613$ $a_2 = 1.355$ $a_3 = 1.355$ $a_4 = 0.613$	(108.3, 0.0, 0.0)
	C_s(IV)	$g_x = 2.0023$ $g_y = 2.0037$ $g_z = 2.0062$	$a_1 = 1.355$ $a_2 = 0.613$ $a_3 = 0.613$ $a_4 = 1.355$	(71.7, 0.0, 0.0)

[a] A denotes principal values of axially symmetric hf tensors and a denotes isotropic hf couplings. [b] The Euler angles (α, β, γ), associated with each site is given with respect to an 'averaged' structure. The anisotropic g-value components were chosen to obtain the smallest g-value, g_z, along the oxygen p_z-orbital (perpendicular to the C–O–C moiety), and the largest, g_x, along H_{eq}–C–O–C–H_{eq}. The Euler angles correspond to *ca.* ± 6° twisting along the C_2 axis and bending the C–O–C moiety along the x-axis. The principal components of the g-tensor were obtained from simulations of the rigid THF cation shown in Fig. 7.

is 'forbidden' in each case). Simulations for non-degenerate structures were attempted but it was found to give too many unknown input parameters (rates) in the modelling. Thus, in order to determine a model unambigiously one must take some of the kinetic and thermodynamic parameters from other kinds of experiment or by calculation.*

Simulations following (*i*) and (*ii*) are shown in Fig. 5(*a*) and (*b*), respectively. Comparing the two models, the main difference in the simulated spectra is the relative amplitudes, particularly for the outer lines compared with the central one. The experimental spectra for $[^2H_8]THF^+$ in CF_3CCl_3 are clearly much better reproduced by the simulations following (*i*). The comparison with the spectra obtained using $CFCl_3$ is less obvious, indeed, similarities are found in both cases. The comparison with experimental spectra is here complicated by the appearance of an additional splitting (discussed in an earlier section) due to ^{19}F as the temperature increases.

The exchange rates of model (*i*) for the CF_3CCl_3 matrix are plotted against reciprocal temperature in Fig. 6. The activation energy which can be calculated (slope) is essentially the same as that obtained from the two-site model (Fig. 4). In the figure is drawn a line associated with an activation energy of 1.7 kcal mol^{-1}.

It is here again pointed out that further refinement of the Arrhenius plot can be achieved by introducing several processes by lifting the accidental degeneracy of C_2 (C_2') and C_s (C_s') imposed by models (*i*) and (*ii*). With the energy difference between C_2 and C_s becoming non-zero and with different barriers on going from C_2 to C_2', or C_s to C_s', *etc.*, at least four independent exchange rates must be determined for each spectrum (each associated with an activation energy). It is, however, impossible to decide these parameters in a unique way without having further information than the hyperfine parameters given by the EPR (or ENDOR) spectrum in the rigid limit.

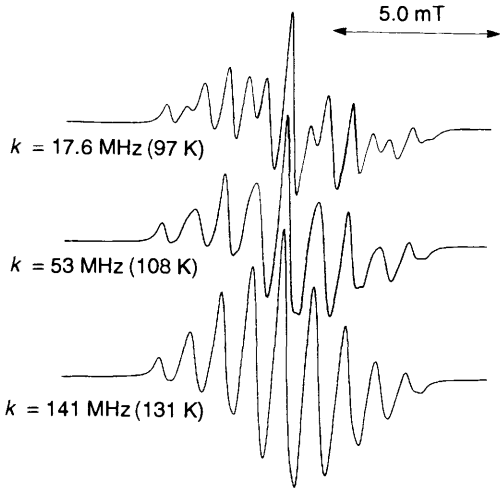

Fig. 4 Simulated EPR spectra of the perdeuteriated THF radical cation in CF_3CCl_3 according to a two-site model. The hyperfine and g-tensor parameters are given in Table 2. The anisotropic hyperfine parameters are switched between the two sites, with the angle between site I and II being 60°, *i.e.*, ± 30° with respect to the unique axis. The anisotropic parameters obtained were chosen to obtain 'the best fit', that is, without taking into account molecular or electronic structure.

The g-tensor used in the four-site model, as well as giving final proof of the assignments, was obtained by simulating the protonated THF cation radical in the CF_3CCl_3 matrix at the rigid limit. The spectra are shown in Fig. 7, where a C_2 structure

* Higher accuracy in the modelling is of course obtained if the hf-interactions are more anisotropic.[10b,10c] The anisotropy of the hfc tensors dominating the line shape of the tetrahydrofuran cation is about 5%, see details concerning the simulation in Fig. 7.

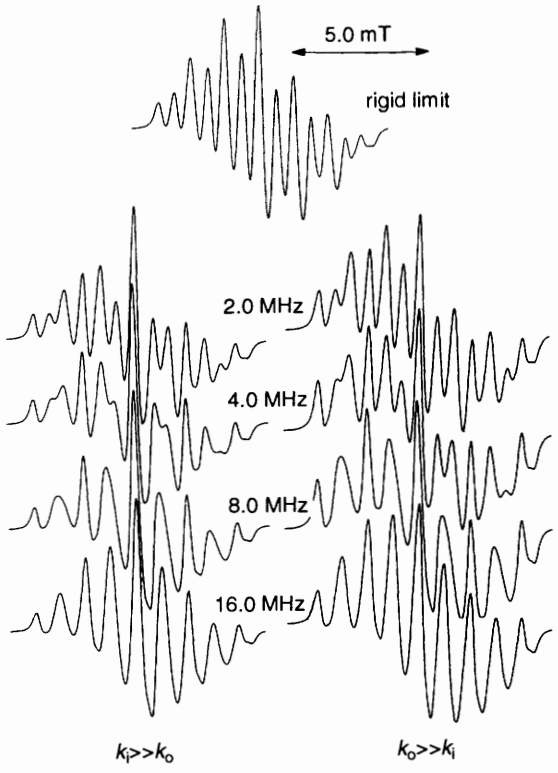

Fig. 5 Simulated EPR spectra of the perdeuteriated THF radical cation in CF_3CCl_3 adopting four sites; the two different models are explained in the text. The EPR parameters used for the different sites are given in Table 2.

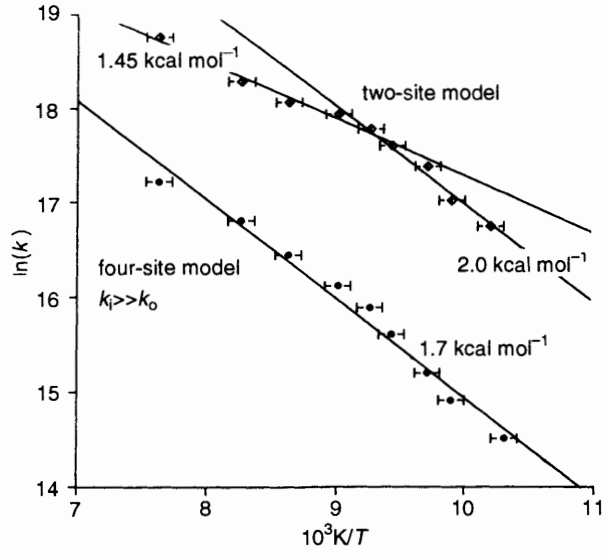

Fig. 6 Arrhenius plots of the exchange rates associated with the two-site and four-site models as explained in the text. The error bars correspond to the uncertainty in the temperature reading of ± 1 K

is assumed.[1]* The parameters used in the simulations are given in Table 1.

Conclusions

This study presents experimental EPR and ENDOR data of the perdeuteriated THF radical cation in the CF_3CCl_3 and $CFCl_3$ matrices. It shows the possibility of combining EPR and ENDOR spectroscopy to studies of matrix (freon) stabilised cation radicals using perdeuteriated solute molecules. EPR is appropriate for the analysis of molecular dynamics and electronic states of the molecule directly through line-shape simulations. ENDOR is shown to give further details of the rigid structure.

The results are analysed by standard methods. The temperature-dependent line-shape of the perdeuteriated THF radical cation is studied by using several models involving two- and four-site jumping. The radical cation is concluded to take a twisted structure in both matrices. From the modelling of the dynamics it is concluded that the molecule exchanges between two C_s and/or two C_2 structures in the CF_3CCl_3 matrix with an activation energy of *ca.* 1.7 kcal mol.$^{-1}$ This is nearly the same value as reported by Shida *et al.*[1] for the protonated analogue in $CFCl_3$, 1.65 kcal mol^{-1}, using a two-site model.

* The symmetry is important when defining the relationship between the hf tensors.

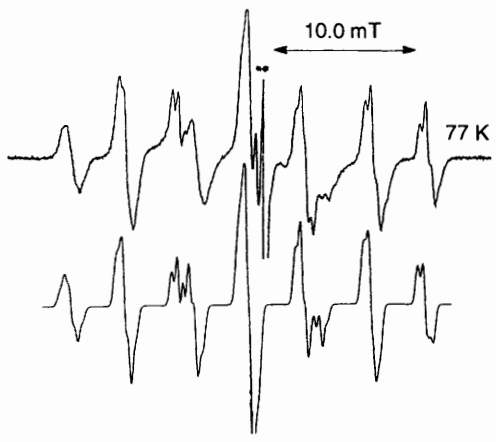

Fig. 7 Experimental (77 K) and simulated (rigid limit) spectra of the THF radical cation (fully protonated). The associated hf and *g*-tensor parameters are given in Table 1.

References

1 H. Kubodera, T. Shida and K. Shimokoshi, *J. Phys. Chem.*, 1981, **85**, 2583.
2 T. Shida, Y. Nosaka and T. Kato, *J. Phys. Chem.*, 1978, **82**, 695.
3 I. G. Smith and M. C. R. Symons, *J. Chem. Res.* (*S*), 1979, 382.
4 T. Wang and Ff. Williams, *J. Phys. Chem.*, 1980, **84**, 3156.
5 M. Iwasaki, K. Toriyama and K. Nunome, *J. Am. Chem. Soc.*, 1981, **104**, 3591.
6 For reviews, see: (*a*) T. Shida, E. Haselbach and T. Bally, *Acc. Chem. Res.*, 1984, **17**, 180; (*b*) M. C. R. Symons, *Chem. Soc. Rev.*, 1984, 393; (*c*) M. Shiotani, *Magn. Reson. Rev.*, 1987, **12**, 333; (*d*) *Radical Ionic Systems*, eds. A. Lund and M. Shiotani, Kluwer, 1991.
7 (*a*) F. Gerson and X.-Z. Qin, *Chem. Phys. Lett.*, 1988, **153**, 546; (*b*) J. Westerling and A. Lund, *Chem. Phys.*, 1990, **140**, 421.
8 (*a*) L. Sjöqvist, A. Lund and J. Maruani, *Chem. Phys.*, 1988, 125, 293; (*b*) L. Sjöqvist, M. Lindgren and A. Lund, *Chem. Phys. Lett.*, 1989, **156**, 323; (*c*) L. Sjöqvist, N. P. Benetis, A. Lund and J. Maruani, *Chem. Phys.*, 1991, **156**, 457
9 (*a*) J. Heinzer, *J. Mol. Phys.*, 1971, **22**, 167; (*b*) J. Heinzer, *QCPE*, Program No. 209, 1972.
10 (*a*) N. P. Benetis, D. J. Schneider and J. H. Freed, *J. Magn. Reson.*, 1989, **85**, 275; (*b*) N. P. Benetis, M. Lindgren, H.-S. Lee and A. Lund, *Appl. Magn. Reson.*, 1990, **1**, 267; (*c*) N. P. Benetis, L. Sjöqvist, A. Lund and J. Maruani, *J. Magn. Reson.*, 1991, **95**, 523.

Paper 3/01984E
Received 30*th March* 1993
Accepted 4*th June* 1993